Bull Earthquake Eng (2011) 9:1417–1442
DOI 10.1007/s10518-011-9278-y

ORIGINAL RESEARCH PAPER

Site response studies and seismic microzoning in the Middle Aterno valley (L'aquila, Central Italy)

G. Lanzo · F. Silvestri · A. Costanzo · A. d'Onofrio · L. Martelli · A. Pagliaroli · S. Sica · A. Simonelli

Received: 25 January 2011 / Accepted: 13 April 2011 / Published online: 3 May 2011

Abstract Following the April 6th, 2009 Abruzzo mainshock, the Italian Civil Protection Department promoted a multidisciplinary study aimed at developing seismic microzonation maps for post-earthquake reconstruction planning. In the framework of this project, a Working Group, including the authors, was assembled to carry out a microzonation study on six villages located in the Middle Aterno valley. This paper focuses on the villages of Castelnuovo and Poggio Picenze, which experienced MCS intensity values of IX–X and

G. Lanzo (✉)
Dipartimento di Ingegneria Strutturale e Geotecnica, University La Sapienza, Rome, Italy
e-mail: giuseppe.lanzo@uniroma1.it

F. Silvestri · A. d'Onofrio
Dipartimento di Ingegneria Idraulica, Geotecnica e Ambientale, University Federico II, Naples, Italy
e-mail: francesco.silvestri@unina.it

A. d'Onofrio
e-mail: anna.donofrio@unina.it

A. Costanzo
Dipartimento di Difesa del Suolo, University of Calabria, Rende, Italy
e-mail: acostanzo@dds.unical.it

L. Martelli
Servizio Geologico, Sismico e dei Suoli, Regione Emilia Romagna, Bologna, Italy
e-mail: lmartelli@regione.emilia-romagna.it

A. Pagliaroli
CNR-IGAG, Rome, Italy
e-mail: alessandro.pagliaroli@uniroma1.it

S. Sica · A. Simonelli
Dipartimento di Ingegneria, University of Sannio, Benevento, Italy
e-mail: stefsica@unisannio.it

A. Simonelli
e-mail: alsimone@unisannio.it

VIII–IX, respectively. 1D and 2D linear equivalent site response analyses were carried out on representative geological cross-sections through the damaged centres and the expansion zones. The subsoil models resulting from geological, geotechnical and geophysical investigations were calibrated by comparing numerical amplification functions, in the linear range, with horizontal-to-vertical spectral ratio derived from both aftershocks and noise recordings. The input motions adopted for the analyses were five artificial accelerograms compatible with three response spectra obtained from the Italian seismic code, as well as from ad hoc probabilistic and deterministic studies. The results were expressed in the form of horizontal profiles of amplification factors in terms of peak ground acceleration, F_{PGA}, as well as of the Housner intensity, FH, in two different range of periods; this latter parameter was shown to be almost independent of the input motion and allowed to express the dependency of site amplification on the frequency range. The amplification factors computed along the representative geological sections were finally extended with a rational procedure to the surrounding areas to draw Grade-3 microzonation maps.

Keywords Aterno River valley · Soil amplification · Dynamic properties · Numerical analyses · Microzonation maps

1 Introduction

About 2 months after the April 6th, 2009 Abruzzo earthquake ($M_w = 6.3$), the Italian Civil Protection Department (DPC) started a comprehensive Seismic Microzonation study on about 30 towns located along the Aterno River valley which experienced an intensity equal to or greater than VI MCS (Galli and Camassi 2009). The whole area was subdivided into 9 macro-zones, and for each one of them the study was committed to a different interdisciplinary working group aggregating several Italian universities and research institutions.

The three-level approach originally introduced by TC4-ISSMGE (1999) and adopted by DPC guidelines (Working Group MS 2008) was followed for the whole area, to support the local municipalities for urban planning of reconstruction in both damaged and expansion zones. For sake of timeliness, Grade-2 mapping was skipped; Grade-1 maps were produced on the basis of geological and geomorphological surveys, addressed to identify and classify 'stable' and 'potentially unstable' areas, the former intended as the zones where neither subsoil failures are present nor significant permanent deformations are expected to occur under earthquake shaking, the latter being the zones subjected to different forms of instability, such as slope failure or liquefaction. Detailed Grade-3 microzonation maps were based on comprehensive geotechnical and geophysical surveys, and on accurate numerical analyses of seismic ground response, aimed at quantifying by appropriate parameters the expected level of soil amplification induced by scenario earthquakes in stable areas. The whole study was fulfilled within less than one year after the earthquake.

A working group, including the authors, was charged to produce Grade-1 and Grade-3 microzonation maps of a macrozone consisting of six villages located in the Middle Aterno valley, 12 to 25 km far from the epicentre (Fig. 1): Petogna ($I_{MCS} = VI$), S. Martino ($I_{MCS} =$ VI–VII), Barisciano ($I_{MCS} = VI$), San Pio delle Camere ($I_{MCS} =$ V–VI), Poggio Picenze ($I_{MCS} =$ VIII–IX), Castelnuovo ($I_{MCS} =$ IX–X). The paper illustrates the subsoil modelling and the results of numerical simulations of site response analyses which leaded to the Grade-3 microzonation maps for the two mostly damaged villages of Poggio Picenze and Castelnuovo.

2 Geological setting and damage at poggio picenze and castelnuovo

For the relatively limited variation of epicentral distances and building stocks, the significant difference noted in the inter-village intensity in the macrozone was attributed mainly to seismic site amplification effects (Lanzo et al. 2010). As a matter of fact, the villages of Petogna, San Martino, Barisciano and San Pio delle Camere suffered a lower damage (I_{MCS} = V to VII), and are mostly settled on stiff rock deposits outcropping at the flank of the slopes bordering the valley; on the other hand, Castelnuovo and Poggio Picenze experienced higher intensity values (I_{MCS} = VIII to X), attributed to their site conditions, characterised by the widespread presence of softer soil deposits. Moreover, the historical chronicles report that both villages suffered a comparable very high intensity (I_{MCS} = X) during the historical 1,461 earthquake; this latter showed source characteristics very similar to the 2009 event, since the epicentre was located in the same area, and the energy was characterised by about the same moment magnitude, estimated as high as M_w = 6.5 (Rovida et al. 2009). Note that in 1,461 the intensity felt at L'Aquila was again I_{MCS} = IX, just like in this last event, and lower than that at Poggio Picenze and Castelnuovo.

The town of Poggio Picenze (695–760 m a.s.l.) lies along a gentle slope located on the left bank (north side) of the Aterno valley, about 14 km away from the instrumental epicenter (Fig. 1).

In spite of the regular morphology of the surface, the subsoil is characterized by stratigraphic variability for the presence of faults affecting the bedrock and giving rise to horst and graben (Fig. 2a, b, c). South of the town, a pop-up structure borders a graben about 1.1 km wide, limited toward north by the calcareous slopes (Miocene calcarenites, indicated with 'M') of the M. Camarda ridge. This graben was filled, during the Pleistocene, by white carbonate silts ('L') of lacustrine origin, belonging to the San Nicandro formation (Bosi and Bertini 1970), and alluvial conglomerates ('cglp'). Locally, in the hollows and at the base of the slopes, debris covers ('d', 'a3') lie on the fluvio-lacustrine deposits. Conglomerates grow thin toward north, where white carbonate silts directly outcrop.

Fig. 1 Geographical location of Poggio Picenze and Castelnuovo with respect to the epicentral area

The building damage at Poggio Picenze was observed to be stronger in the historical center, where most masonry constructions including a monumental church (Fig. 2d) were heavily damaged, while nearby RC buildings were almost unaffected by the shaking (Fig. 2e). The geological map and cross-sections in Fig. 2a, b, c show that this part of the town mostly lies on a thick layer (up to 50 m) of a white carbonate silts. Minor damage was detected in

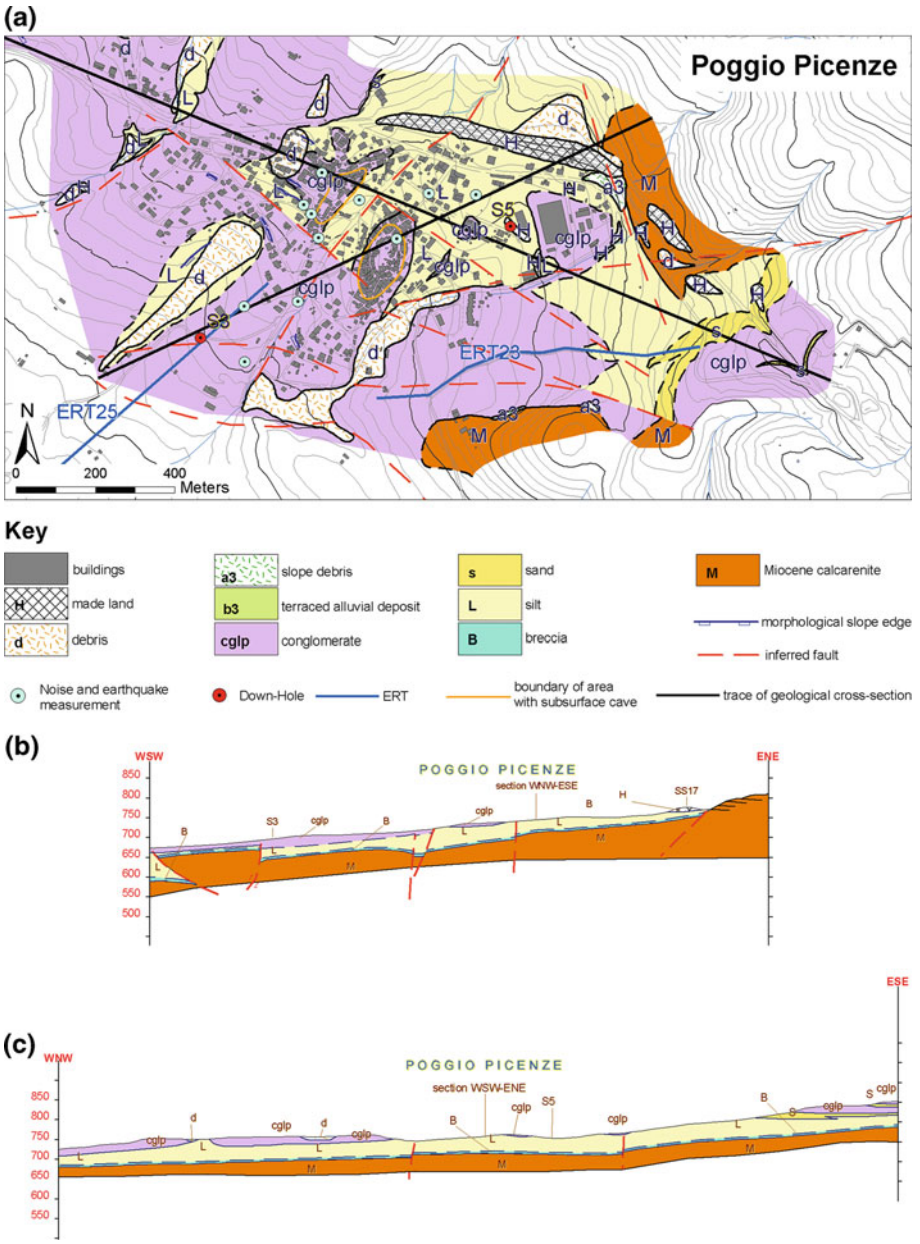

Fig. 2 Poggio Picenze: Geological map (**a**) and cross-sections (**b, c**); variable degree of damage (**d, e**)

Fig. 2 continued

the western and downhill parts of the town; these areas are settled on some tens of meters of a Pleistocene conglomerate, overlying a comparable thickness of white silts. In the area near the castle several holes were observed in the street floor, caused by the collapse of the roof of underground caves; these latter, probably of natural origin, have been enlarged in the years and used as cellars.

The village of Castelnuovo (810–860 m a.s.l.) lies about 22 km away from the epicenter (Fig. 1). The old village is settled on an elliptical hill, elongated in the NW–SE direction and rising 60 m above the surrounding alluvial plain.

The whole hill is constituted by the white carbonate silt of lacustrine origin ('L', Fig. 3a, b, c), engraved by the Aterno river during Late Pleistocene age. Late Pleistocene terraced alluvia ('b3') fill-in the topographic lows of the plain, surrounding the eastern and southern sides of the village; at the toe of the hill, a shallow Holocene detrital cover ('d') overlaps the contact between the lacustrine silt and the alluvial formation.

The bedrock plunges gradually toward south; therefore the thickness changes of the fluvio-lacustrine deposits, predominantly white silt, are mostly conditioned by the surface morphology.

The building stock, partly inhabited, is mainly constituted by un-reinforced masonry structures 2–3 stories in height; some of the structures were retrofitted with through-going iron bars, apparently following the intense damage ($I_{MCS} = VIII$) suffered during the strong Avezzano earthquake in 1915 (estimated $M_W = 7$).

Shaking was strong enough to significantly damage almost the entire village, with most of the structures on the top and in the upper half of the hill either collapsed or close to collapse (Fig. 3d). A lower damage level was observed on the buildings at the toe of the hill (Fig. 3e); these latter, however, pertain to a more recent construction period and should therefore be less vulnerable. In Castelnuovo old village, just as observed at Poggio Picenze, holes occurred in the street floor due to collapses of the roof of caves.

Summarising, in both towns the subsoil is mainly characterised by the constant presence of the lacustrine white silt formation, which is locally termed as 'Creta bianca'.

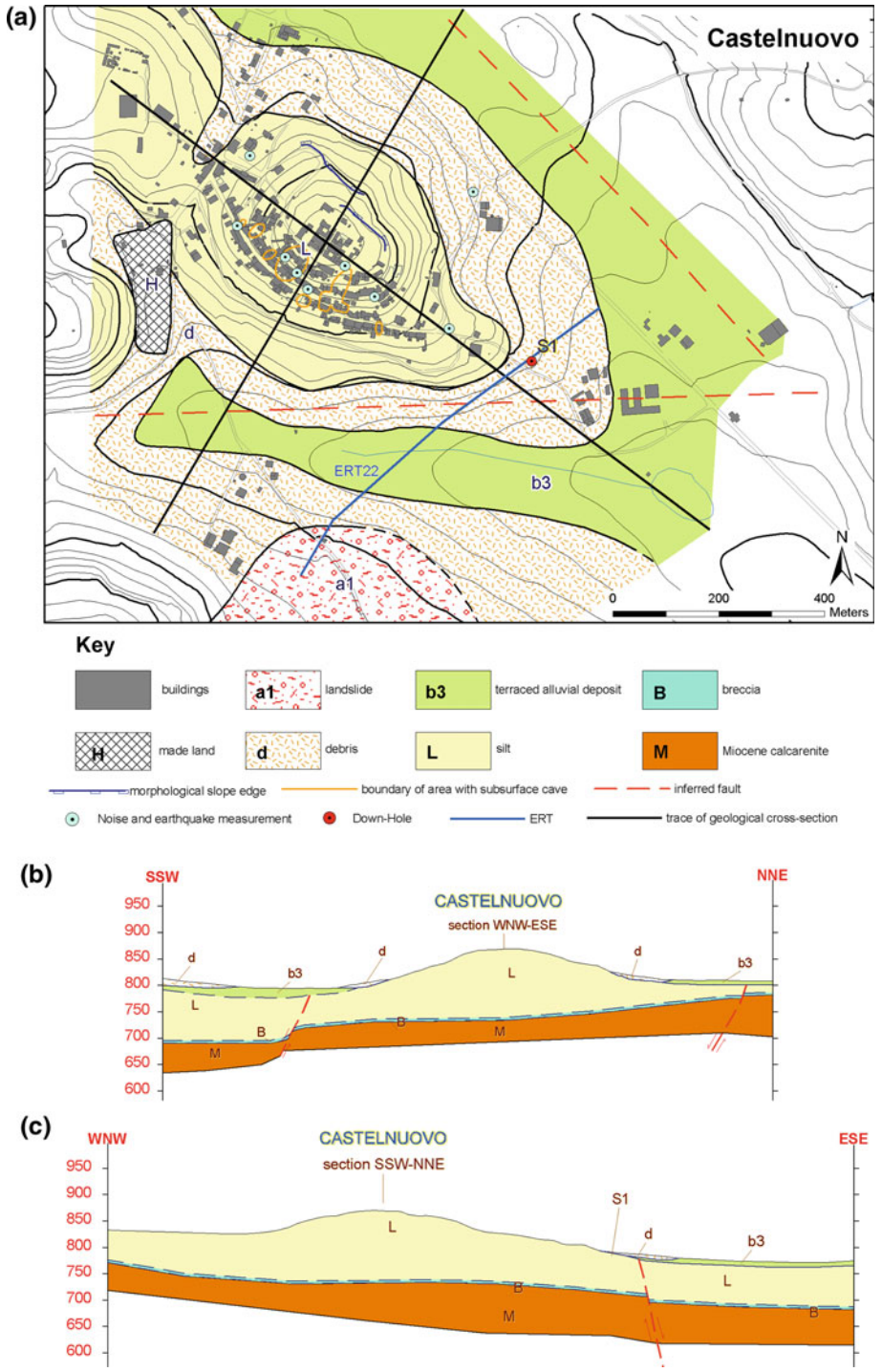

Fig. 3 Castelnuovo: Geological map (**a**) and cross-sections (**b, c**); variable degree of damage (**d, e**)

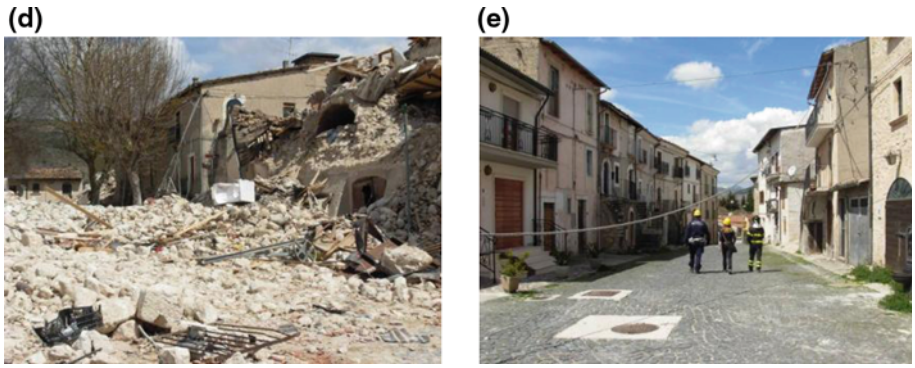

Fig. 3 continued

From several investigations in the broader area, it was deduced that a few meters of continental breccia (termed as 'B' in Figs. 2 and 3) are deposited at the base of the white silts, on the underlying stiff bedrock made of Miocene limestone ('M').

3 Geotechnical characterisation

The geometry of the geo-lithological sections shown in Figs. 2 and 3 was mainly based on the results of geological and geophysical surveys, and calibrated on the basis of boreholes, specifically executed for the seismic microzonation of the area. These data were integrated with few stratigraphic logs already available from previous investigations. It should be noted that none of the boreholes, drilled to a maximum depth of 50 m, intercepted the seismic bedrock; this was assumed as corresponding to the Miocenic calcarenites, the depth and geometry of which was defined on the basis of the geological setting of the area reported in literature (Bosi and Bertini 1970), and confirmed by three deep geo-electric tomography surveys (ERT), drawn in Figs. 2a and 3a with blue lines. It will be shown in the following that these assumptions were calibrated on the measurements of noise and aftershocks of the seismic sequence.

In the site-specific investigations carried out in in the macrozone, the groundwater was never individuated. Existing information from water collector wells indicated that the phreatic surface was found in the bedrock formation only (Working Group 2011).

The seismic response analyses adopted the traditional visco-elastic linear-equivalent approach; therefore, the geotechnical model of the subsoil (Table 1) required the characterisation of each material in terms of unit weight, γ, shear and compression wave velocity, V_S and V_P, and the variation of shear modulus and damping ratio with shear strain, $G(\gamma)$ and $D(\gamma)$.

The S-wave velocities of the different soils were mostly determined from Down Hole and MASW tests carried out in the macro-zone (Working Group 2011). For each lithological unit, the values of V_P and Poisson's ratio ν reported in Table 1 were obtained by averaging α (i.e., the ratio V_P/V_S) throughout the different depth ranges explored by DH tests. These parameters were then used for 2D seismic response analyses.

Site-specific laboratory tests were carried out on undisturbed block samples of the Creta Bianca carbonate silt (clay fraction ranging between 28 and 38%, plasticity index 11–19%)

Table 1 Physical and mechanical properties of the different materials for the site response analyses

Soil	Layer	γ (kN/m^3)	V_S(m/s)	ν	α	V_P(m/s)
d	0–15 m	18	250	0.39	2.32	580
shallow debris	15–40 m	18	350	0.38	2.26	790
b3	0–5	18	200	0.38	2.27	455
terraced alluvial	5–10 m	18	300	0.36	2.14	641
deposits	> 10 m	18	400	0.37	2.22	890
cglp	cglp-w: weathered (0–10 m)	20	400	0.39	2.35	942
Pleistocene	cglp-c: cemented (10–25 m)	21	1,000	0.33	2.01	2,008
conglomerate	cglp-c: cemented (>25 m)	22	1,250	0.33	2.01	2,509
L	0–50 m	18	300 + 3.6z	0.38	2.27	681 + 8.2z
Lacustrine white	50–90 m	18	480 + 2.5 (z-50)			1,090 + 5.7 (z-50)
carbonate silts	90–200 m	18	580 + 0.2 (z-90)			1,317 + 0.5 (z-90)
B						
breccia	5 m	21	800	0.36	2.13	1,701
M (bedrock)		22	1,250	0.33	2.01	2,509
Miocene calcarenites						

taken from excavation cuts located in both towns (Working Group 2011). For the other formations, the main physical and mechanical properties were collected from laboratory tests previously carried out on borehole samples of similar soils, retrieved outside the macrozone in the Aterno valley (d'Onofrio et al. 2010).

Figure 4 shows the typical soil layering and V_S profiles retrieved from two DH tests at Poggio Picenze (Fig. 4a) and Castelnuovo (Fig. 4b). The S wave velocities are plotted as resulting from the equivalent travel time (t_s), measured every 2 m, and from the dromochrone, referring to the entire soil layer.

The mean values of the shear wave velocity measured in the debris (unit d, see Fig. 4b) did not exceed 300 m/s and showed a slight variation with depth. Based on the results of further DH tests carried out in the macrozone (see Working Group 2011; Bilotta et al. 2011), a shear wave velocity profile slightly increasing with depth, from about 200 m/s at surface to about 400 m/s at depth greater than 10 m, was assigned to the terraced alluvial deposit (b3 in Table 1).

The DH tests carried out on the Pleistocene conglomerates (cglp) showed a remarkable sensitivity of the shear wave velocity to the variable degree of bonding with depth, due to the weathering (Fig. 4a). They have therefore been characterized by V_S increasing from 400 m/s for the weathered shallow layer (cglp-w) to 1,000–1,250 m/s for the cemented deep layer (cglp-c).

The values of V_S measured in the white carbonate silt deposit, due to the lacustrine origin, showed a significant increase with depth (unit L, see Fig. 4b) which cannot be adequately represented by a constant mean value, like that represented by the dromochrone in Fig. 4b.

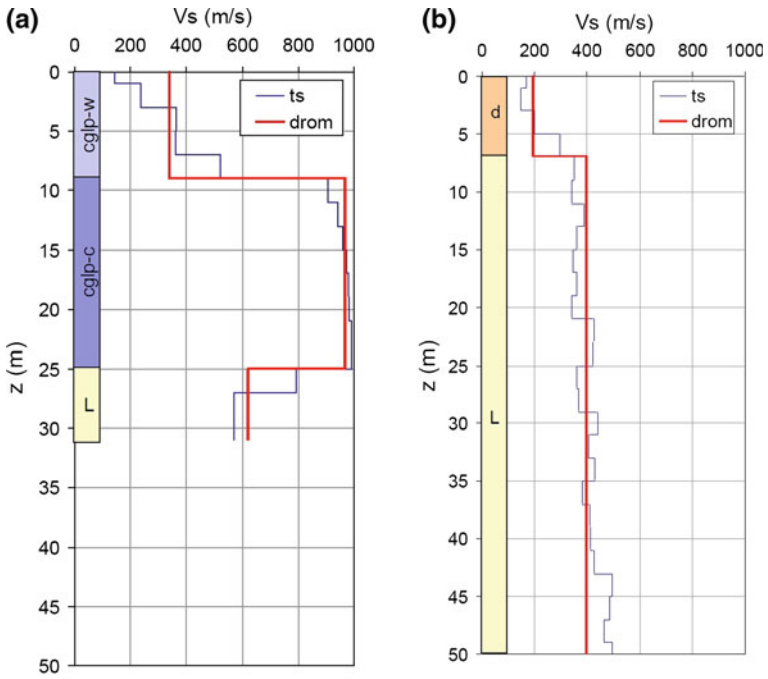

Fig. 4 Soil layering and DH profiles in two test sites: S3 at Poggio Picenze (**a**) and S1 at Castelnuovo (**b**)

On the basis of the whole set of measurements collected in the various DH tests carried out in the macrozone, the dependence of V_S on depth was modelled with a linear law down to 50 m, i.e. the maximum depth explored in the DH tests (Fig. 5). The increase of V_S at higher depth was described by scaling the law of variation of the small strain shear stiffness, G_0, with the mean effective stress, p', measured in resonant column (RC) tests carried out at the University of Naples on the undisturbed block samples (Working Group 2011). The resulting V_S profile is a piecewise linear function with a slope decreasing with z (see Table 1, Fig. 5), which, extrapolated to the maximum depth of 200 m, reaches a value around 600 m/s.

The geophysical tests carried out in the macrozone did not allow the direct measurement of shear wave velocity in the breccia (B) deep transition layer and in the underlying calcareous bedrock (M). The V_S values used in the analyses (see Table 1) were therefore assumed on the basis of measurements taken at other sites located in the Aterno valley, outside the macrozone under study, where such formations are shallower (Working Group 2011). In particular, the shear wave velocity of the bedrock was taken equal to that measured by a down-hole test at the AQV seismic station of the national accelerometric network, located in the upper Aterno valley (Di Capua et al. 2009).

The non-linear and dissipative properties adopted for the numerical analyses are plotted in Fig. 6, in terms of variation with shear strain of the normalised shear modulus, $G(\gamma)/G_0$, and damping ratio, $D(\gamma)$. The figure shows the significant variability of the curves relevant to the different materials, characterised by a wide variation of grain size and structure.

The non-linear behaviour of the "Creta Bianca" silt (L) was determined by cyclic torsional shear (CTS) tests carried out at a frequency of 0.5 Hz on the above mentioned undisturbed

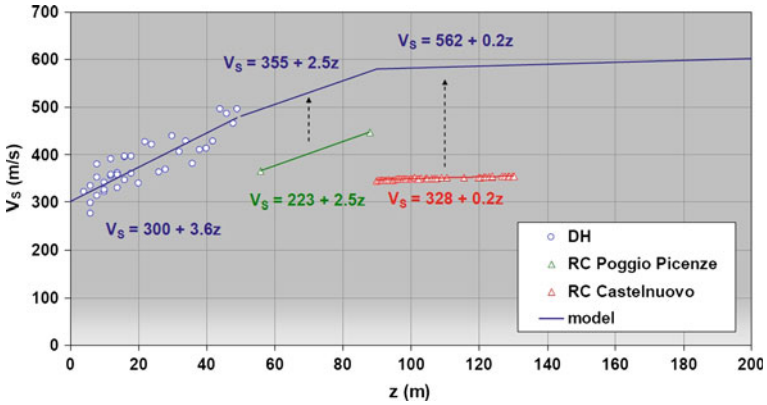

Fig. 5 Variation of shear wave velocity with depth for the white carbonate silts from field and laboratory tests

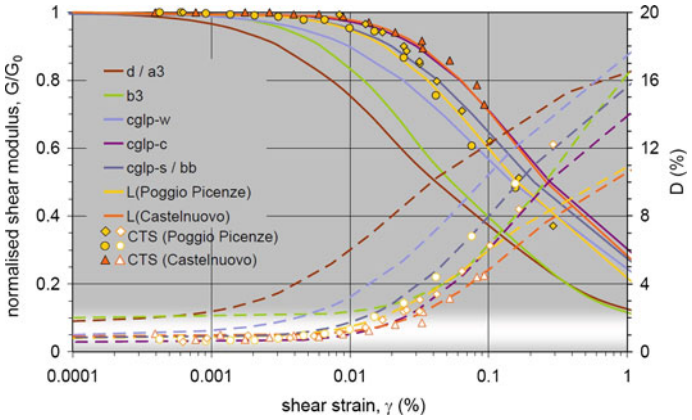

Fig. 6 Non-linear behaviour of the soils

block samples. The experimental results are plotted in Fig. 6 with full and open symbols for $G(\gamma)/G_0$ and $D(\gamma)$, respectively. It can be noted that the sensitivity of stiffness and damping to the strain level results more pronounced for the samples taken at Poggio Picenze than for that at Castelnuovo.

The curves for the terraced alluvia (b3) were taken from cyclic/dynamic laboratory tests carried out on borehole samples of comparable sandy soils in the Aterno valley (d'Onofrio et al. 2010). The non-linear properties of the remaining soils were assigned by referring to literature data on similar materials.

In particular, the non-linear properties of the debris (d) was assigned through literature curves measured on gravelly soils (Rollins et al. 1998; Anh Dan et al. 2001). Different non-linear characteristics of stiffness and damping were assumed for the conglomerates, according to the degree of weathering and bonding. For the weathered shallow layer (cglp-w), the recent work of Modoni and Gazzellone (2010) on dense gravel was taken as a reference; while the curves for the cemented material layer (cglp-c) were taken from previous analysis

on Apennine formations with similar lithology (Costanzo 2007). The non-linear properties of the deep breccia layer (B) were assumed as intermediate between those of the weathered and cemented conglomerates. The bedrock was modelled as a linear material, with a very small value of damping ratio ($D_0 = 0.5\%$).

4 Input motions

Reference input motions for numerical analyses were provided by an ad hoc Working Group formed up by the Department of Civil Protection within the microzonation project (Working Group 2011; Pace et al. 2011). The working group adopted three alternative hazard approaches to derive three reference acceleration response spectra: probabilistic, deterministic and the recent National Technical Code (Ministero delle Infrastrutture e dei Trasporti 2008). The probabilistic study allowed the definition of an uniform hazard spectrum (UHS) corresponding to a return period T_r of 475 years. The same probabilistic study lead to a disaggregation analysis which yielded a single conservative reference pair of magnitude ($M_W = 6.7$) and distance ($R_{epi} = 10$ km) values for all the sites involved in the microzonation project. Thus, in the deterministic approach, a reference median spectrum was obtained from the Sabetta and Pugliese (1996) ground motion prediction equation, based on the same magnitude-distance pair. Finally, the smooth spectrum of the National Technical Code (NTC) corresponding to a return period of 475 years, i.e. that corresponding to the limit state of life safety for ordinary buildings, was also considered.

The same working group made available a set of five acceleration time histories for the numerical analyses, two compatible respectively with the UHS and the NTC spectra, while the remaining three matching the deterministic spectrum. It was not possible to reconstruct a reference input motion on the basis of natural accelerograms, due to the lack in the whole area of any reliable strong-motion record taken on a flat rock outcrop; therefore, all the selected accelerograms were artificial. The two accelerograms matching the NTC and the UHS spectra were obtained via a hybrid procedure from real accelerograms conveniently modified in order to satisfy the compatibility with the target spectrum (Sanò 2011); the other three accelerograms were generated by the SIMNOST code (Sabetta and Pugliese 1996). A more detailed description of the procedure followed for the definition of the reference earthquake input motion to be used for numerical simulations can be found in Pace et al. (2011).

Taking into account the large extension of the sections used for the 2D analyses, in order to limit the mesh element size, the frequency of 15 Hz was selected as the maximum value to be transmitted. As a consequence, the accelerograms compatible with the UHS and NTC spectra were pre-processed with a Butterworth low-pass filter of order 4 and a cut-off frequency of 15 Hz. Conversely, no filtering was applied to the deterministic accelerograms, because they were characterized by negligible frequency content above 15 Hz.

Figure 7 shows the five accelerograms (det1, det2, det3, prob and NTC) used for the study, while the corresponding elastic acceleration response spectra (5% structural damping) are illustrated in Fig. 8; in the same figure the NTC spectra, as specified by the Italian code for target performance levels of Life Safety (SLV, $T_r = 475$ years) and Collapse Prevention (SLC, $T_r = 975$ years) are also plotted for comparison.

PGA values vary between 0.22 g (NTC) and 0.38 g (det3) while the maximum spectral amplification ranges between 0.6 g (NTC) and 1.1 g (prob,det1). The response spectrum of the accelerogram associated with the probabilistic hazard approach (prob) is characterized by the highest ordinates, about twice higher than those of the SLV NTC spectrum. The response spectra of the deterministic accelerograms (det1, det2 and det3) are overall intermediate

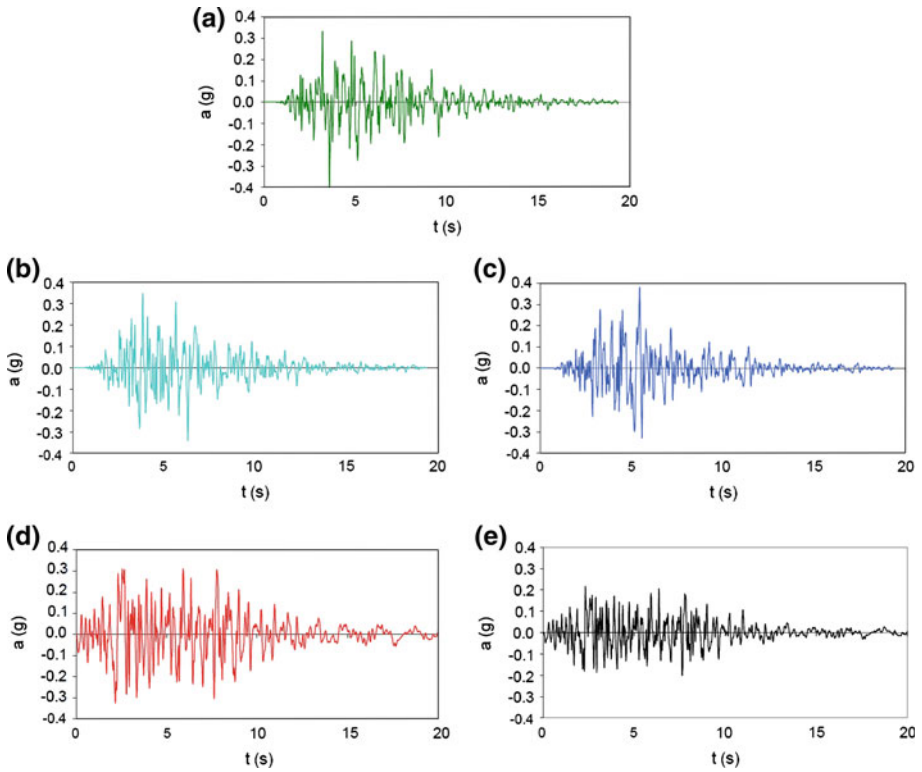

Fig. 7 Input accelerograms resulting from different hazard analyses: Deterministic (**a, b, c**), probabilistic (**d**) and compatible with the spectrum specified by the National Code, return period = 475 years (**e**)

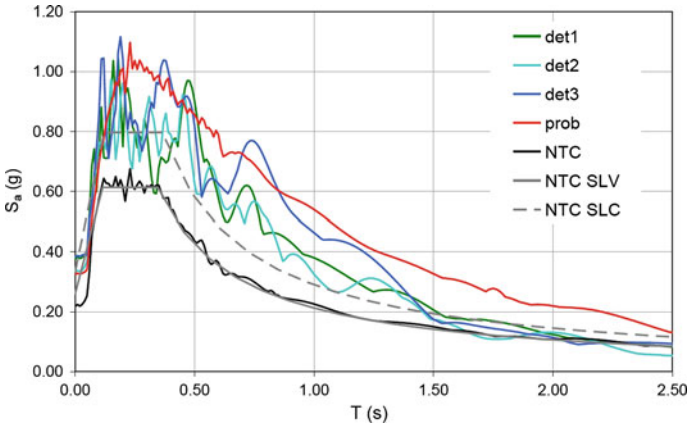

Fig. 8 Acceleration spectra of the input motions versus those specified by the National Code

between the NTC and UHS spectra. It is worth noting that also the SLC NTC spectrum is generally characterized by lower spectral ordinates than those from probabilistic or deterministic accelerograms.

5 Seismic response analysis

5.1 Poggio Picenze

Seismic response analyses were carried out along the two cross-sections shown in Fig. 2b, c. Section WSW-ENE was investigated by 2-D FEM analyses through the code QUAD4M (Hudson et al. 1994), which operates in the time domain. Along section WNW-ESE the layering is quite more regular: therefore, 2D analyses were considered useless or, at least, oversized, and seven representative soil columns were analysed by the 1-D code EERA (Bardet et al. 2000), working in the frequency domain. In both cases, soil response was modelled by the equivalent linear procedure, implementing the curves $G/G_0 - \gamma$ and $D\text{-}\gamma$ described in Fig. 6.

The QUAD4M analyses were carried out by assuming vertically incident SV waves as input motion. The code reproduces the radiation damping by introducing viscous dampers at the bottom of the mesh (absorbing boundaries). By contrast, side boundaries are perfectly reflecting; therefore, in order to reduce the influence of artificial reflected waves, side boundaries were extended about 500 m in both directions from the region of interest. The maximum thickness of mesh elements, h_{max}, for all materials was fixed according to the indication by Kuhlemeyer and Lysmer (1973):

$$h_{\max} \leq \frac{V_S}{8 f_{\max}} \tag{1}$$

being V_S the shear wave velocity value selected according to the shear strain level. As already said, the maximum frequency to be transmitted, f_{max}, was assumed equal to 15 Hz, due to the sampling rate and the low-pass filtering of the seismic input signals. The aspect ratio of the elements (i.e. the width divided by the thickness) was set not greater than 3.

As above mentioned, in the castle area, caves, probably of natural origin then enlarged and used as cellars, do exist (Fig. 2a). These caves were not included in the numerical model because no accurate information was available about their shape, elongation and dimensions. Anyway, it should be considered that, assuming $f_{max} = 15$ Hz, the wavelength propagating through conglomerates and carbonate silts should not be lower than 20 m and therefore seismic waves do not interact significantly with cavities having dimensions smaller than few meters (1–3 m).

To validate the subsoil models assumed for the numerical study, linear analyses were initially carried out to compare the horizontal-to-vertical spectral ratio (HVSR) amplifications obtained experimentally (Working Group 2011) to numerical transfer functions; these latter were computed as the ratio between the smoothed Fourier spectrum in the node of interest and the corresponding spectrum of input motion. Soil behaviour was assumed to be visco-elastic with mechanical properties characterized by their small strain values. Figure 9 shows, for both sections, the comparisons between the numerical transfer functions and the HVSR computed from microtremors (PPCZ04, POG2 and POG4 sites) or weak-motion events (MI28 and VGFZ03 sites). In each plot the 1D and 2D numerical transfer functions are plotted as continuous lines, while the experimental results are represented by a shaded area corresponding to the frequency range where the HVSR ratio is higher than 2, as required by the clarity criterion specified by SESAME (2004).

The fundamental frequencies from measurements fall in the range 2–3 Hz for most stations. The transfer functions computed by both 1D and 2D numerical analyses generally show the fundamental frequency in the amplification range measured experimentally.

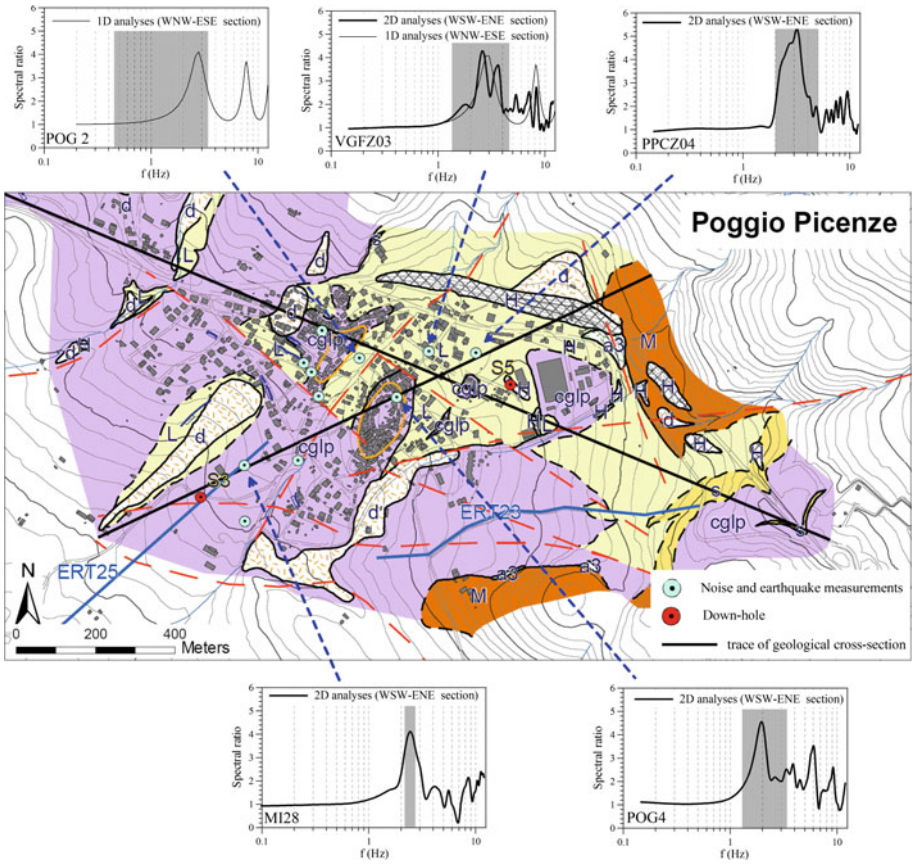

Fig. 9 Comparison between the linear frequency response computed by the numerical model (*continuous line*) and the ranges recorded on microtremors and aftershocks (*shaded area*) at Poggio Picenze

The overall good match between experimental and numerical transfer functions corroborates the subsoil models employed for the seismic response analyses.

The surface amplification resulting from numerical analyses is illustrated in Figs. 10, 11 for sections WSW-ENE and WNW-ESE, respectively. In these figures, the horizontal profiles of amplification factors for PGA (F_{PGA}, Figs. 10a, 11a) and Housner intensity computed in the period ranges 0.1–0.5s ($FH_{0.1-0.5s}$, Figs. 10b, 11b) and 0.7-1.3s ($FH_{0.7-1.3s}$, Figs. 10c, 11c), are plotted for the five selected input accelerograms. Figures 10d, 11d compare the average profiles of the three amplification factors F_{PGA}, $FH_{0.1-0.5s}$ and $FH_{0.7-1.3s}$, which represent the high, intermediate and low frequency amplification effects, respectively.

The amplification factor F_{PGA} is strongly dependent on the seismic input, especially where the silt formation outcrops or is covered by thin layers of conglomerate (e.g., between 650 and 1,350 m in Fig. 10a). By examining the average profiles along both sections (Figs. 10d and 11d), F_{PGA} is lower on the conglomerate cover and increases where the silt formation dominates, reaching peak values of 3 along WSW-ESE section (see Fig. 10d at a distance of about 1,000 m) and 2 along the WNW-ESE section (see Fig. 11d at a distance of about 1,100 m). F_{PGA} values around 2 or slightly lower were computed where conglomerate and silt layers of comparable thickness (of the order of 50–70 m overall) overlay the bedrock (e.g., between 225 and 500 m in Fig. 10d). Values of F_{PGA} around 1.5 were obtained where

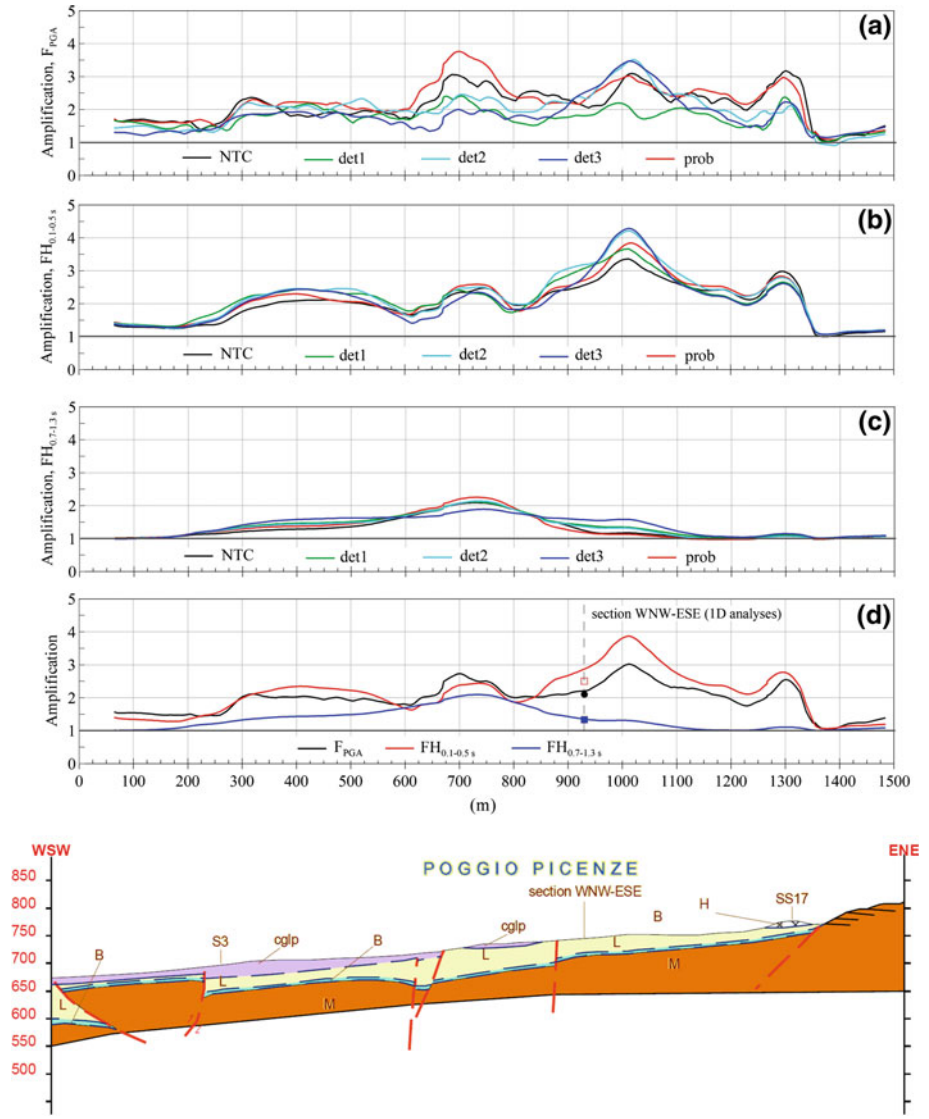

Fig. 10 Horizontal profiles of amplification factors in terms of PGA (**a**) and Housner intensity in the period range 0.1–0.5 s (**b**) and 0.7–1.3 s (**c**), computed for the five different seismic inputs by 2D analyses along WSW-ENE section at Poggio Picenze. In (**d**) comparison among the average profiles of the three amplification factors

the bedrock is closer to the ground surface, being the conglomerate-silt cover thinner than 20 m (between 50 and 225 m in Fig. 10d).

The results in terms of Housner intensity from 2D (Fig. 10b, c) and 1D (Fig. 11b, c) analyses highlight that FH is poorly sensitive to the input motion, in both intermediate and low frequency ranges. Along both sections, the average $FH_{0.1-0.5s}$ values are generally higher than average F_{PGA} (see Figs. 10d, 11d). The only exceptions occur where the conglomerate-silt cover is thin (50–225 m in Fig. 10d) and where the silt layer is thicker

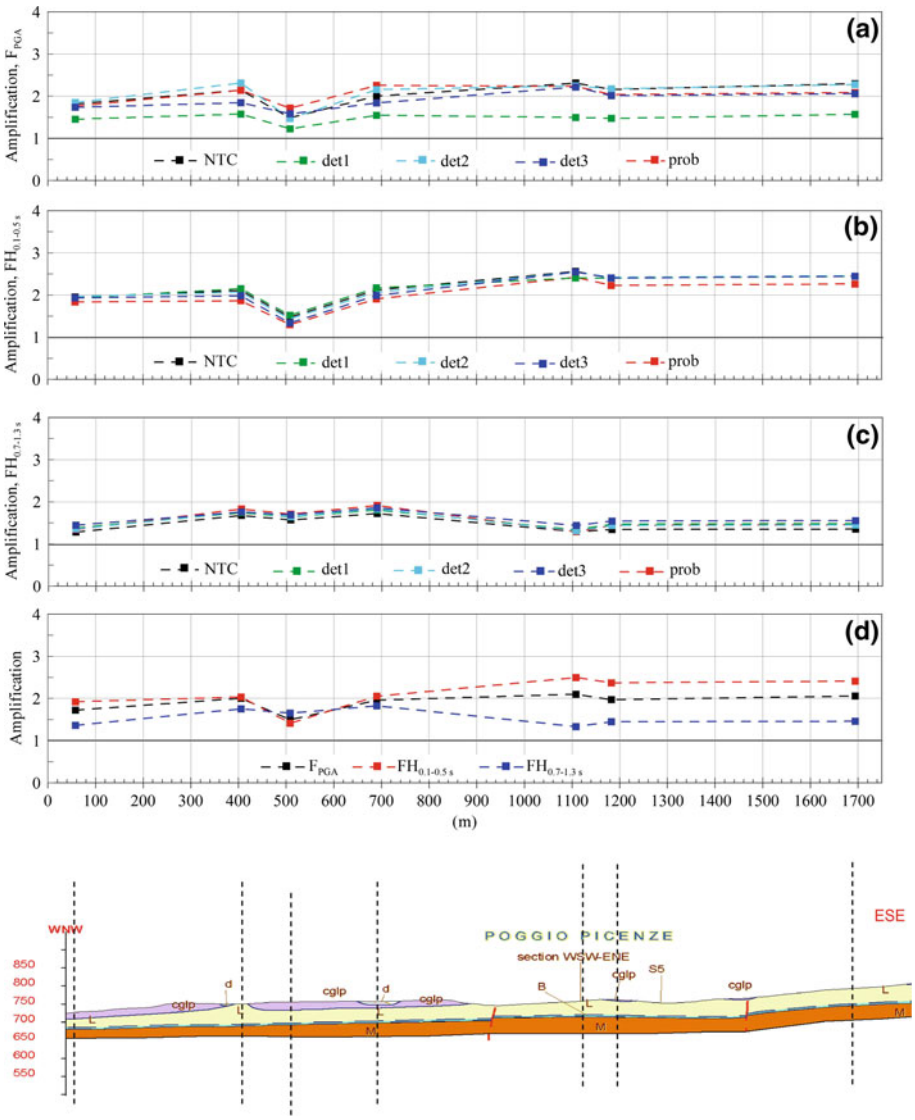

Fig. 11 Horizontal profiles of amplification factors in terms of PGA (**a**), Housner intensity in the period range 0.1–0.5 s (**b**) and 0.7–1.3 s (**c**), computed for the five different seismic inputs by 1D analyses along WNW-ESE section at Poggio Picenze. In (**d**) comparison among the average profiles of the three amplification factors

(600–850 m in Fig. 10d). The highest amplification factors (3–4) were predicted at distances 950–1,050 m along section WSW-ENE, where a 30 m-thick silt layer overlies the bedrock (Fig. 10d). Resonance and 2D phenomena, including interference between surface waves generated at the edge of bedrock and direct volume waves, can be figured out to explain such high amplification values, as the 1D modelling provides $FH_{0.1-0.5\,s} \approx 2.5$ for comparable stratigraphic conditions (see Fig. 11d at distance 1,125 m).

The average low-frequency amplification factor $FH_{0.7-1.3s}$ values are significantly lower than both F_{PGA} and $FH_{0.1-0.5s}$ along both sections (Figs. 10d, 11d). The peak values, around 2, are located in the range distance 600–850 m along WSW-ENE section (Fig. 10d), where the silt thickness is maximum (50–70 m).

Figure 10d also shows the comparison between 2D (continuous line) and 1D analysis (scattered points) where the two sections intersect (at a distance around 925 m). The agreement in terms of F_{PGA} is quite satisfactory, and appears even better for both $FH_{0.1-0.5s}$ and $FH_{0.7-1.3s}$.

In sum, largest amplification factors are generally associated with the Housner intensity parameter calculated in the period range 0.1–0.5 s ($FH_{0.1-0.5\,s}$). This circumstance can be explained by observing that the fundamental period of the silt deposit falls usually between 0.3 and 0.5s (i.e. 2–3 Hz) in the linear range. It increases to 0.4–0.65 s (1.5–2.5Hz) if a reduction of 40% of G with respect to G_0 is assumed due to non-linearity, since $G/G_0 = 0.60$ roughly corresponds to the maximum shear strain $\gamma = 0.1\%$ computed for the carbonate silt in the site response analyses. Therefore, maximum amplification effects were duly expected for $FH_{0.1-0.5s}$ because of possible resonance phenomena. Conversely, for analogous reasons, the lowest amplification factors were generally found for Housner intensity parameter calculated in the period range 0.7–1.3s (0.77–1.4 Hz). Moreover, along both sections the $FH_{0.7-1.3s}$ of the silt deposit is observed to increase with the thickness of the soil layer and hence proportionally to the fundamental period.

5.2 Castelnuovo

The numerical 2D simulations of the seismic response of the Castelnuovo hill were carried out along the two sections shown in Fig. 3b, c, by means of the FLAC 5.0 (Itasca 2005) code, operating in the time domain with the finite difference method (FDM). Such code was preferred to QUAD4M for its capability to reliably model adsorbing lateral boundaries, since in this case the bedrock outcrops too far from the hill. The soil behavior was assumed as linear equivalent visco-elastic, with non-linear stiffness and hysteretic damping controlled by sigmoidal functions, calibrated on the curves $G/G_0 - \gamma$ and $D\text{-}\gamma$ reported in Fig. 6. The small strain damping ratio, D_0, was included in the FDM algorithm according to the well-known Rayleigh formulation, where the coefficients were chosen following a double frequency approach (Hashash and Park 2002; Lanzo et al. 2003), yielding the same damping-frequency function as the single frequency method used by the program (Costanzo 2007).

The two mesh grids used to model the geological sections were characterized by thickness of the elements set equal to 4 m in order to reproduce a maximum frequency of about 15 Hz according to the rule by Kuhlemeyer and Lysmer (1973). The aspect ratio of the elements was set not greater than 3.

To avoid undesired wave reflections, a ‘quiet boundary’ condition was adopted for the bedrock (Lysmer and Kuhlemeyer 1969), consisting of viscous dampers acting along normal and tangential directions, whereas ‘free-field boundary’ conditions were used for the lateral contours. These latter consist of one-dimensional columns simulating the behaviour of a lateral semi-infinite medium, linked to the mesh grid through viscous dashpots.

As for Poggio Picenze, cavities existing at hilltop beneath the old village (Fig. 3a), were not included in the numerical models.

Figure 12 shows the comparison between the HVSR, obtained by microtremor signals recorded along the hill of Castelnuovo (Working Group 2011), and the numerical transfer functions from the linear visco-elastic analyses carried out on both sections. Transfer functions were computed as the ratio between the smoothed Fourier spectrum obtained at the

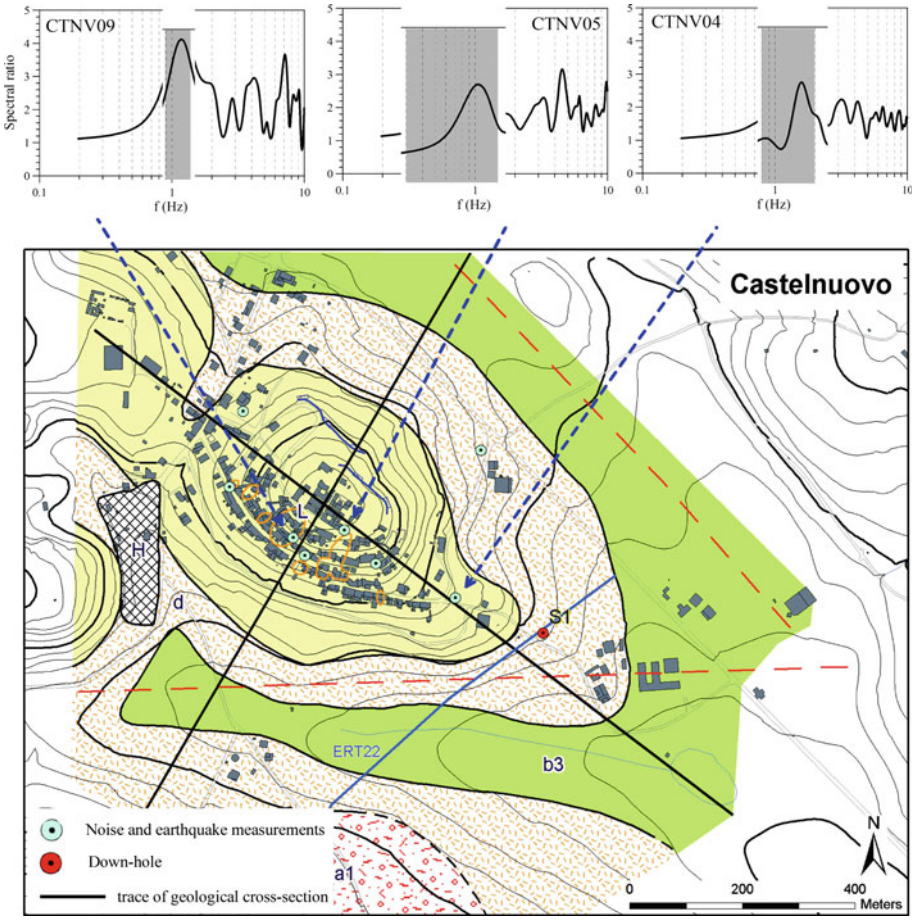

Fig. 12 Comparison between the linear frequency response computed by the numerical model (*continuous line*) and the ranges recorded on microtremors (*shaded area*) at Castelnuovo

hilltop and that of the input motion. All microtremors records taken in the historical centre at the hilltop (sites CNTV01, CNTV05, CMTV09) indicated a fundamental frequency of the hill of about 1 Hz. The numerical amplification functions for both sections show an overall good agreement with the instrumental data, thus validating the subsoil model assumed for the analyses.

Figures 13 and 14 show the amplification factors along the sections WNW-ESE and SSW-NNE, respectively, in terms of PGA (Figs. 13a, 14a) and Housner intensity, again computed in the period ranges 0.1–0.5 s (Figs. 13b, 14b) and 0.7–1.3s (Figs. 13c, 14c); the profiles of the above factors, averaged for the five input accelerograms, are compared in Figs. 13d and 14d.

The amplification factor in terms of PGA (F_{PGA}) results, once more, strongly dependent on the seismic input, especially where the shallow cover of alluvial or debris deposits overlies the silt formation at the toe of the hill (i.e. at distances 950–1,400 m in Fig. 13a, 0–450 m and 850–1,150 m in Fig. 14a). The peak values of F_{PGA} are predicted at the NNE side of the

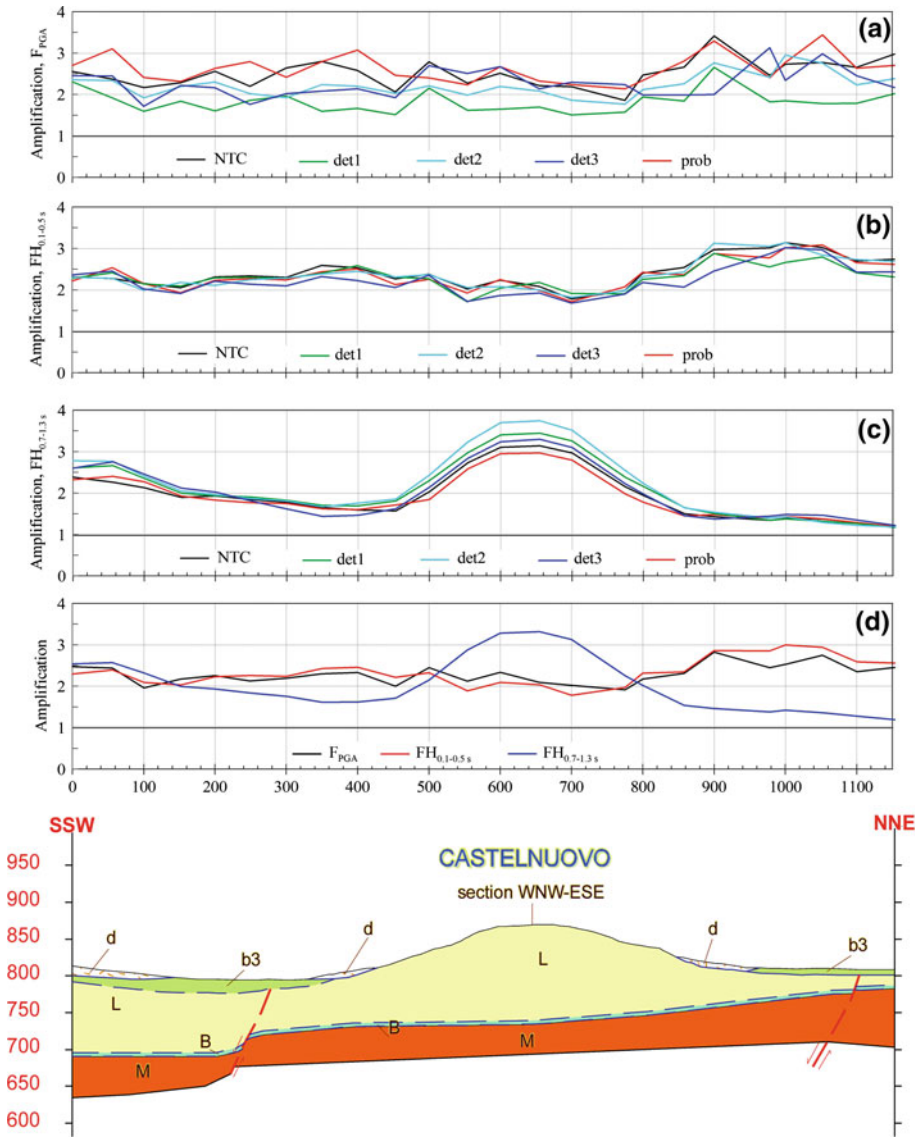

Fig. 13 Horizontal profiles of amplification factors in terms of PGA (**a**) and Housner intensity in the period range 0.1–0.5 s (**b**) and 0.7–1.3 s (**c**), computed for the five different seismic inputs by 2D analyses along SSW-NNE section at Castelnuovo. In (**d**) comparison among the average profiles of the three amplification factors

hill (see Fig. 14a–d) where the thickness of the carbonate silt plus the shallow cover is lower than 20 m; instead, along the slopes and at the hilltop, the F_{PGA} values are quite irregular not showing any particular trend. Their average values plot steadily around 2.0 along the longitudinal section (WNW-ESE, see Fig. 13d), and range between 2.0–2.5 along the transversal section (SSW-NNE, see Fig. 14d).

The trends of the horizontal profiles in Figs. 13b, c and 14b, c confirm that the amplification factors in terms of Housner intensity show a lower scatter with the different input motion

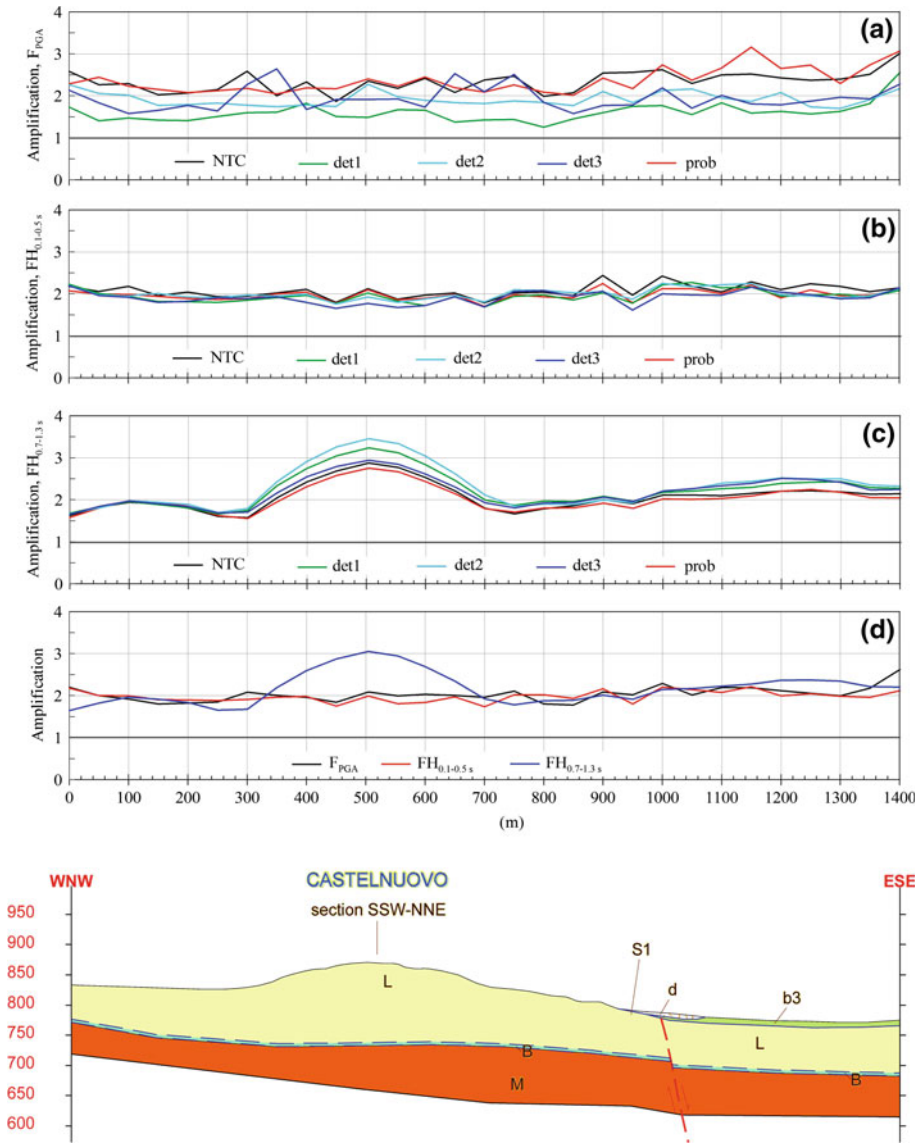

Fig. 14 Horizontal profiles of amplification factors in terms of PGA (**a**) and Housner intensity in the period range 0.1–0.5 s (**b**) and 0.7–1.3 s (**c**), computed for the five different seismic inputs by 2D analyses along WNW-ESE section at Castelnuovo. In (**d**) comparison among the average profiles of the three amplification factors

if compared to F_{PGA}, like the Poggio Picenze case. However, their variations are significantly different according to the frequency range considered.

Along the whole longitudinal direction of the elliptical hill, the intermediate frequency amplification factor ($FH_{0.1-0.5s}$) shows very small variations around 2.0, with average values very close to F_{PGA} (Fig. 13d). The same factor generally assumes values higher than 2 along the transversal section, being inversely proportional to the bedrock depth, and increasing to

even about 3 in the NNE zone, where the bedrock upraises and the thickness of the silty layer is lower (Fig. 14d).

It may appear singular that both F_{PGA} and $FH_{0.1-0.5s}$ profiles show their lowest values at the hilltop along both sections, which could lead to the conclusion that the influence of the topographic amplification is minor with respect to the stratigraphic effects, at least in the intermediate to high frequency range (i.e. f > 2Hz). This can be justified considering that the characteristic frequencies recorded along of the hill are of the order of 1 Hz (see Fig. 12), thus falling inside the range represented by the low-frequency amplification factor $FH_{0.7-1.3s}$. As a matter of fact, the horizontal profiles of this parameter show trends similar to the topographic profile. Figures 13c, d and 14c, d highlight that $FH_{0.7-1.3s}$ is lower than 1.5 where the silt layer is less than 50m thick, while on the hilltop the average amplification of motion results equal to or greater than 3. Along both sections the low-frequency amplification factor $FH_{0.7-1.3s}$shows an opposite trend with respect to F_{PGA} and $FH_{0.1-0.5s}$. In this frequency range, therefore, the seismic response of the Castelnuovo hill appears predominantly affected by topographic amplification.

6 Seismic microzonation maps

On the basis of the numerical analyses, the Grade-3 zoning of the seismic response was carried out. Since in both villages no unstable areas (landslides, liquefiable soils, etc.) were identified, the seismic microzonation maps coincide with the distributions of the amplification factors.

The maps have been constructed by extrapolating and interpolating the results of the seismic response calculated along the cross-sections. As shown by the horizontal profiles of amplification factors computed along the cross-sections (Figs. 10, 11, 13, 14) the fluctuations of the amplification factors result strictly correlated to the variability of local geological conditions. A rational procedure was adopted to draw the contours of microzonation maps, by first bracketing the horizontal profiles with upper bound values of amplification factors; then, the microzones were mapped after areal extrapolation and interpolation among cross-sections of the above values, on the basis of the local stratigraphic variations. These were identified as the significant changes in depth of the most important stratigraphic unconformities (e.g., the contact between bedrock and white silt) and thickness of the quaternary bodies (conglomerate, white silt, etc.), as well as tectonic displacements (most of all faults) producing significant changes either in depth of unconformities or in thickness of the lithostratigraphic units. Thus, boundaries between microzones correspond to changes of amplification factors and local subsoil conditions (stratigraphic variations and/or faults), derived from the geological maps and cross-sections. On the other hand, each microzone identifies an area with fairly constant amplification value and homogeneous stratigraphic and tectonic conditions.

Considering the most common construction typology of existing and new buildings, the spectral amplification factor $FH_{0.1-0.5s}$ was assumed as the most significant parameter for both reconstruction and urban planning. Therefore, the seismic microzonation maps were drawn in terms of average values of $FH_{0.1-0.5s}$ with respect to those calculated for the five different input motions. For Castelnuovo, where instrumental records shown strong amplifications for frequencies around 1 Hz, a map of $FH_{0.7-1.3s}$ was also proposed.

The amplification maps shown in Figs. 15, 16 and 17 are briefly described hereafter. A colour palette ranging from blue for no amplification (FH=1.0), yellow to orange tones ($1.0 < FH < 2.0$) and red to purple tones ($FH > 2.0$) was adopted with a resolution of 0.1, according to the standards specified by the Italian Civil Protection Department. Areas with

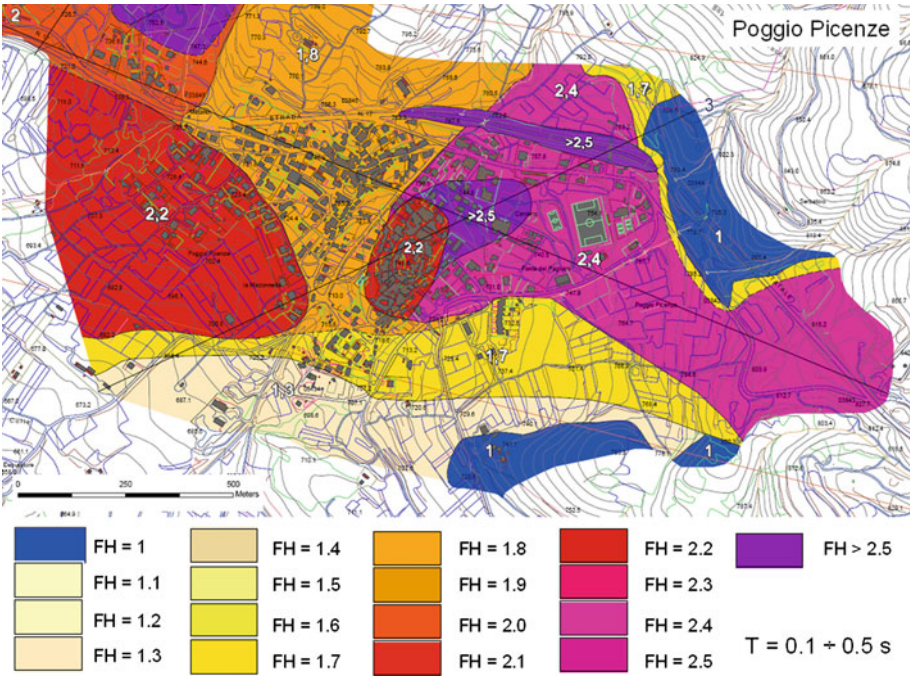

Fig. 15 Seismic microzonation map of Poggio Picenze in terms of $FH_{0.1-0.5\,s}$

amplification value > 2.5 were represented with the same purple colour, without distinction of the local value.

6.1 Poggio Picenze

North and south of the village, either bedrock outcrops or areas with thin (< 3 m) debris layers are present. In these areas, the numerical analyses did not point out any significant amplification and $FH_{0.1-0.5s} = 1$ was assumed (Fig. 15).

Where the thickness of the debris cover is higher than 3 m, the amplification factor always resulted >1. The spectral amplification factor increases where the conglomerate thickness decreases, attaining values always greater than 2, and sometimes even higher than 2.5, where the Quaternary deposit is made by white silt.

Values as high as 2.2 were assigned to the conglomerate slab in the whole castle area, which is particularly critical also for the presence of the natural caves (see Sect.2 and Fig. 2a). Values of $FH_{0.1-0.5s}$ always higher than 2.5 were also estimated throughout the embankment along the main road SS17 (see also Fig. 10).

6.2 Castelnuovo

The numerical analyses showed quite high amplification values for this area. Everywhere $FH_{0.1-0.5s}$ is in fact at least equal to 1.9 (Fig. 16), with the maximum value attained in the plain northeast of the hill, where $FH_{0.1-0.5s}$ is higher than 2.5 on the alluvial and debris cover.

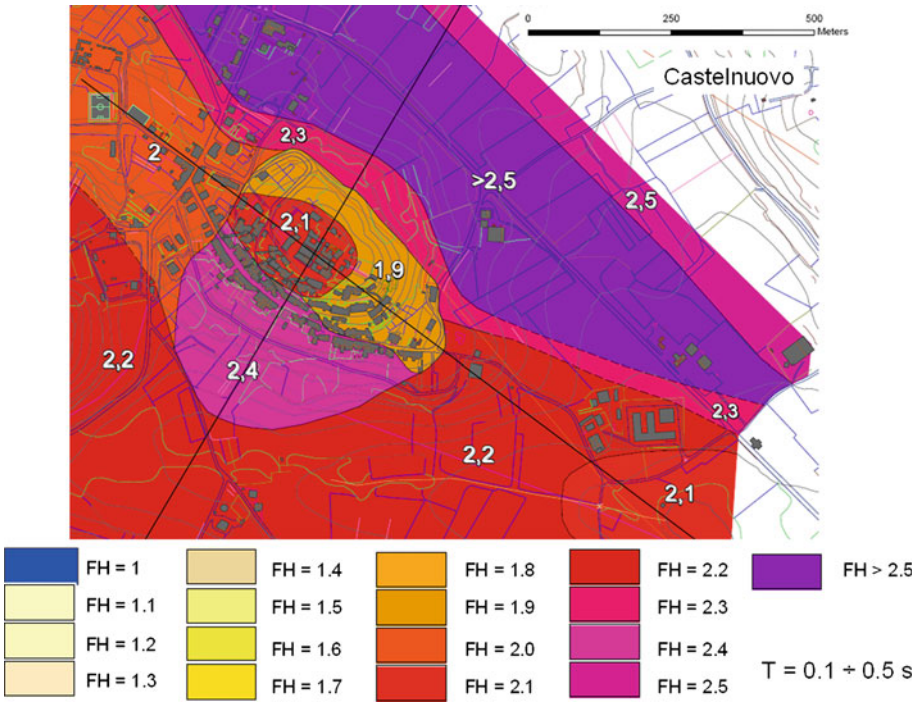

Fig. 16 Seismic microzonation map of Castelnuovo in terms of $FH_{0.1-0.5\,s}$

On the other hand, the map relevant to $FH_{0.7-1.3s}$ (Fig. 17) confirms the evidences of the instrumental records, i.e. that the maximum amplification, for frequencies around 1 Hz, occurs on the top of the hill and in the WNW and ESE plain, along a direction coinciding with the longitudinal axis of the relief and of the valley. Along the transverse direction (NNE-SSW), the value of $FH_{0.7-1.3s}$ decreases from more than 2.5 at the top of the hill, to 1.9 on the alluvial and debris cover at the SSW flank, and down to 1.4 in the NNE plain, where the thickness of the white silt is less than 100 m.

As in the Poggio Picenze castle area, a critical aspect of the Castelnuovo old village, at the top of the hill, was the presence of caves (orange circled areas in Fig. 3a) few metres under the surface. Note that this area is characterised by amplification factors $FH_{0.1-0.5s}$ ranging between 1.9 and 2.4, whereas they are higher than 2.5 in the low-frequency spectral amplification map (Fig. 17).

7 Conclusions

The seismic response analyses and microzonation studies carried out at Poggio Picenze and Castelnuovo represent further interesting case studies of seismic risk of small historical towns in the Apennines, following those already analysed by the authors in previous research projects, and summarised by Costanzo et al. (2007).

In both cases, some peculiarities in the subsoil appear to characterise the ground motion predicted at surface under the seismic input motions considered for the microzonation study.

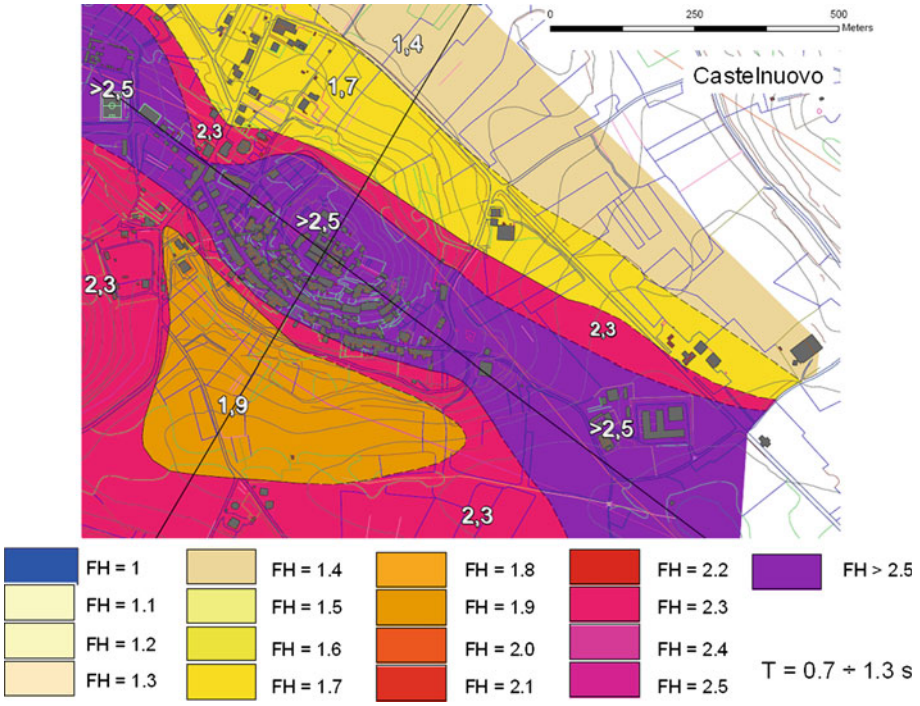

Fig. 17 Seismic microzonation map of Castelnuovo in terms of $FH_{0.7-1.3\,s}$

For both sites, the seismic response is dominated by the geotechnical properties of the deep deposit of white carbonate silts of lacustrine origin, showing stiffness significantly dependent on depth.

More in detail, the site response of the town of Poggio Picenze is mainly conditioned by the irregular morphology of the bedrock and the local presence of weathered conglomerate layers stiffer than the underlying silts. On the other hand, the site amplification predicted along the Castelnuovo hill is strongly conditioned by the variable thickness of the deformable silt deposit, locally covered by thinner debris and alluvial deposits.

In both sites, the predicted amplification at surface was expressed by means of different representative ground motion parameters, which allowed to widely describe the dependency of site amplification on the frequency range considered. The microzonation maps were drawn bounding zones with homogeneous layering and expected values of amplification factors in terms of Housner intensity, FH. The choice of such parameter allowed an unambiguous identification of the areas affected by higher potential for amplification of ground motion, whatever the seismic input. Moreover, the proposal to compute FH throughout two different ranges of periods may be helpful to predict the likely amplification of seismic motions on buildings and infrastructural systems with different dynamic properties, which can be of straightforward use for the urban planning and the reconstruction phase.

At the same time, the high degree and the non-uniform distribution of damage suffered during the mainshock of April, 6th, 2009 can be rationally explained accounting for the individual influence of site amplification and vulnerability of the existing building stock. To this purpose, an accurate mapping of the building type and degree of damage resulting from

the post-earthquake survey was produced (Working Group 2011), and further studies on the likely influence of cavities on the building damage are currently in progress.

Acknowledgments The study was carried out on behalf of the Italian Civil Protection Department, under the supervision of dr. Giuseppe Naso. All the members of the interdisciplinary working group dealing with 'Macrozone 4' are warmly acknowledged for their contributions.

References

Anh Dan LQ, Koseki J, Tatsuoka F (2001) Viscous deformation in triaxial compression of dense well graded gravels and its model simulation. In: Tatsuoka F (ed) et al Advanced laboratory stress-strain testing of geomaterials. Balkema, The Netherlands, pp 187–194

Bardet JP, Ichii K, Lin CH (2000) EERA a computer program for equivalent-linear earthquake site response analyses of layered soil deposits. University of Southern California, Department of Civil Engineer, US

Bilotta E, Evangelista L, Landolfi L, Silvestri F (2011) Site response analysis for microzonation: a comparison of different numerical approaches and amplification factors. In: Proc. V ICEGE, Santiago.

Bosi C, Bertini T (1970) Geologia della media valle dell'Aterno. Memorie della Società Geologica Italiana, IX, 719–777 (in Italian)

Costanzo A (2007) Analisi di fenomeni deformativi di pendii e rilievi in condizioni sismiche: il caso di Gerace. Ph.D. thesis in geotechnical engineering, University of Calabria (in Italian)

Costanzo A, d'Onofrio A, Lanzo G, Pagliaroli A, Penna A, Puglia R, Santucci De Magistris F, Sica S, Silvestri F, Tommasi P (2007) Seismic response of historical centers in Italy: selected case studies. In: Workshop on 'Geotechnical Earthquake Engineering related to Monuments and Historical Centers', Proc. IV ICEGE, Thessaloniki

Di Capua G, Lanzo G, Luzi L, Pacor F, Paolucci R, Peppoloni S, Scasserra G, Puglia R (2009) Caratteristiche geologiche e classificazione di sito delle stazioni accelerometriche della RAN ubicate a L'Aquila. Project S4, INGV-DPC Agreement 2007–2009. http://esse4.mi.ingv.it/ (in Italian)

d'Onofrio A, Evangelista L, Landolfi L, Silvestri F, Boiero D, Foti S, Maraschini M, Santucci de Magistris F (2010) Geotechnical characterization of the C.A.S.E. project sites. In: Proc. Sustainable Development Strategies for Constructions in Europe and China, Rome

Galli P, Camassi R (eds) Report on the effects of the Aquilano earthquake of 6 April 2009. http://www.mi.ingv.it/eq/090406/quest_eng.html

Hashash YMA, Park D (2002) Viscous damping formulation and high frequency motion propagation in non-linear site response analysis. Soil Dyn Earthq Eng 22:611–624

Hudson M, Idriss I M, Beikae M (1994) Quad4M-A computer program to evaluate the seismic response of soil structures using finite element procedures and incorporating a compliant base. University of California Davis, California

Itasca (2005) FLAC 5.0-user's manual. Itasca Consulting Group, Minnesota

Kuhlemeyer L, Lysmer J (1973) Finite element method accuracy for wave propagation problems. J Soil Mech Found Div 99(SM5):421–427

Lanzo G, Pagliaroli A, D'Elia B (2003) Numerical study on the frequency-dependent viscous damping in dynamic response analyses of ground. In: Proc. of IV Int Conf Earthq Resist Eng Struct (ERES 2003), Ancona

Lanzo G, Di Capua G, Kayen RE, Scott Kieffer D, Button E, Biscontin G, Scasserra G, Tommasi P, Pagliaroli A, Silvestri F, d'Onofrio A, Simonelli AL, Puglia R, Mylonakis G, Athanasopoulos G, Vlahakis V, Stewart JP (2010). Seismological and geotechnical aspects of the Mw=6.3 l'Aquila earthquake in central Italy on 6 April 2009, Int J Geoengin Case Hist 1(4): 206–339. http://casehistories.geoengineer.org

Lysmer J, Kuhlemeyer L (1969) Finit e dynamic model for infinite media. J Eng Mech Div 95(EM4):859–877

Ministero delle Infrastrutture e dei Trasporti (2008) Le Norme Tecniche per le Costruzioni. D.M. 14 gennaio 2008. Gazzetta Ufficiale 29 (supplemento Ordinario 30). http://www.infrastrutture.gov.it/consuplp/

Modoni G, Gazzellone A (2010) Simplified theoretical analysis of the seismic response of artificially compacted gravels. V International conference on recent advances in geotechnical earthquake engineering and soil dynamics, san diego (USA), Paper No. 1.28a

Monaco P, Totani G, Barla G, Cavallaro A, Costanzo A, d'Onofrio A, Evangelista L, Foti S, Grasso S, Lanzo G, Madiai C, Maraschini M, Marchetti S, Maugeri M, Pagliaroli A, Pallara O, Penna A, Saccenti A, Santucci de Magistris F, Scasserra G, Silvestri F, Simonelli AL, Simoni G, Tommasi P, Vannucchi G, Verrucci L (2010) Geotechnical aspects of the L'Aquila earthquake. In: Invited lecture at earthquake geotechni-

cal engineering satellite conference, XVII international conference on soil mechanics and geotechnical engineering, 2-3.10.2009, Alexandria (in press)
Pace B, Albarello D, Boncio P, Dolce M, Galli P, Messina P, Peruzza L, Sabetta F, Sanò T, Visini F (2011) Predicted ground motion after the L'Aquila 2009 earthquake (Italy, Mw 6.3): input spectra for seismic microzoning. Bull Earthquake Eng 9:199–230
Rollins KM, Evans MD, Diehl NB, Daily WDIII (1998) Shear modulus and damping relationship for gravels. J Geotech Geoenvironmental Eng ASCE 124(5):396–405
Rovida A, Castelli V, Camassi R, Stucchi M (2009) Historical earthquakes in the area affected by the April 2009 seismic sequence. INGV report. http://www.mi.ingv.it/eq/090406/storia_eng.html
Sabetta F, Pugliese A (1996) Estimation of response spectra and simulation of nonstationary earthquake ground motion. Bull Seism Soc Am 86(2):337–352
Sanò T (2011) Personal communication
SESAME (2004) Guidelines for the implementation of the H/V spectral ratio technique on ambient vibrations measurements, processing and interpretation. SESAME European research project. WP12 – Deliverable D23.12. http://sesame-fp5.obs.ujf-grenoble.fr/index.htm
TC4-ISSMGE (1999) Manual for zonation on seismic geotechnical hazard (Revised Version). Technical Committee for Earthquake Geotechnical Engineering, TC4, ISSMGE. Japanese Geotechnical Society
Working Group MS (2008). Indirizzi e criteri per la microzonazione sismica. Conferenza delle Regioni e delle Province autonome-Dipartimento della protezione civile, Roma. vol. 3 and Cd-rom.
Working Group (2011) La Microzonazione sismica dell'area aquilana. vol. 3 + dvd. Dipartimento della Protezione Civile-Regione Abruzzo (in Italian) (in press)